

Impedance Characteristics of Oxide Layers on Aluminium

Han-Jun Oh,* Kyung-Wook Jang, and Choong-Soo Chi†

Department of Materials Science, Hanseo University, Seosan 352-820, Korea

†School of Metallurgical and Materials Engineering, Kookmin University, Seoul 136-702, Korea

Received September 20, 1999

The electrochemical behavior of oxide layers on aluminium was studied using electrochemical impedance spectroscopy. Impedance spectra were taken at a compact and a porous oxide layer of Al. The anodic films on Al have a variable stoichiometry with gradual reduction of oxygen deficiency towards the oxide-electrolyte interface. Thus, the interpretation of impedance spectra for oxide layers is complicated, with the impedance of surface layers differing from those of ideal capacitors. This layer behavior with conductance gradients was caused by an inhomogeneous dielectric. The frequency response cannot be described by a single RC element. The oxide layers of Al are properly described by the Young model of dielectric constant with a vertical decay of conductivity.

Introduction

Anodizing is an electrochemical process in which aluminium is converted into aluminium oxide by the application of an anodic current in an anodic environment. When the oxidation on aluminium in aqueous solution produces surface oxide film, the composition and structure of oxide layers vary widely, depending on the conditions of film formation.

In principle, the aluminium oxide formed in H₂SO₄ solution has a complex form. It is partially hydrated and has a twolayer structure. At the surface of the metal, there is a thin, compact boundary layer and then there is a porous overlayer. The latter has a very open structure. In anodizing for ammonium adipate (NH₄OCO(CH₂)₄COONH₄) electrolyte, the oxide layer is a relatively thin compact barrier type¹⁻³ film. In humid air, the pure aluminum forms extremely thin but dense natural oxide layers, these films are generally accepted to consist of a thin amorphous Al₂O₃ layer,^{4,5} which is estimated at about 20 Å to 100 Å in thickness.

For the evaluation of the properties of oxide layers on aluminium, electrochemical impedance spectroscopy (EIS) was used as early as 1962 by Hoar and Wood,⁶ who studied the sealing process of the porous layer. In previous investigations⁷⁻⁹ the properties of anodic oxide films were characterized with electrical equivalent circuits consisting of series and parallel combinations of resistances and capacitances for an ideal parallel plate capacitor. But for anodic oxide films on Al, Ti, Nb and Ta, it is well known that the oxide layer adjacent to the metal-oxide interface is characterized by variable stoichiometry with gradual reduction of oxygen deficiency towards the oxide-electrolyte interface.¹⁰⁻¹² Therefore, the impedance properties of an oxide layer on aluminium in contact with an electrolyte have not been fully described with an equivalent circuit of a simple RC element for an ideal capacitor.

The aim of this work is to investigate the impedance characteristics and the electrochemical behavior of various oxide layers on Al by using equivalent circuit with Young impedance, which is allowed to appropriately interpret the inho-

mogeneous dielectric of oxide layer. For an appropriate interpretation, the microstructure of the barrier type anodic film was compared with the anodic film thickness evaluated by impedance spectra.

Experimental Section

Materials. A sheet of aluminum (99.9 wt%, Tokai Metal Co, Japan) was electropolished in a perchloric acid/ methanol mixture at 20V for 5 min. at 5 °C, then washed in distilled water and finally dried in a cool air stream. After electropolishing, the three types of aluminum oxide film were prepared:

1) The natural aluminum oxide passive film was prepared from exposure in humid air for 10 days at ambient temperature (24-26 °C).

2) The barrier type oxide layer was treated at a constant voltage of 130V in 150 g/L ammonium adipate (NH₄OCO(CH₂)₄COONH₄) electrolyte for 15 min. at 65 °C.

3) The porous oxide layer was anodized at a constant voltage of 22V in 1 M sulfuric acid at 20 °C for 33 min.

After anodizing, the three types of oxide layers were washed and rinsed in distilled water. The three types of oxide layers on aluminum were then prepared for working electrode. The surface of these oxide layers was studied by impedance spectra at 25 °C in 0.5 M K₂SO₄ in an unstirred and aerated solution. All potentials were referenced to the Hg/Hg₂SO₄/0.5 M K₂SO₄ solution in this paper. A platinum plate was used for the counter electrode. The exposed total area of the working electrodes in the electrolyte was 1cm².

Impedance spectroscopy measurements. Impedance spectra were recorded with commercially available equipment (IM6, Zahner-electric, Germany). The computer system integrated into this device was used for measurement and data evaluation. All impedance spectra were plotted against the frequency range. The impedance spectra were measured at open-circuit potential, imposing a low amplitude AC voltage signal of 10 mV. Accordingly, the disturbance of the material electrode system was low enough to

ensure a linear response in the form of an alternating current signal with the same frequency but shifted by phase angle φ with respect to the applied AC voltage. The total complex impedance of the material electrode system is recorded as a function of the applied frequency.

The recorded impedance spectra are treated by

$$\begin{aligned} \ln\{Z(\omega)\} &= \ln\{|Z(\omega)|\} + i\varphi(\omega) \\ \text{or } \log\{Z(\omega)\} &= \log\{|Z(\omega)|\} + i\varphi(\omega) \log e \end{aligned} \quad (1)$$

Since the real part of $\log Z$ according to Eq. (1) is the logarithm of modulus $|Z|$ and the imaginary part is the phase angle φ , it is obvious that Bode diagrams ($\log |Z|$ vs. $\log f$, φ vs. $\log f$) should be used if frequency dependencies are to be represented explicitly. The advantages of Bode plots and the loss of information resulting from Nyquist plots were convincingly demonstrated by Mansfeld.¹³

The measured impedance data were analyzed by a computer simulation and fitting program.^{14,15}

And for comparison with calculated layer thickness from impedance spectra, the microstructure of the oxide layer was examined by transmission electron microscopy (TEM). For the examination of oxide film by TEM, a narrow strip of the barrier type anodized specimen was encapsulated with a mixture of Agar 100 and a hardener for ultramicrotomy. After curing at 60 °C for 24 hours, the embedded specimen was trimmed with a glass knife and then sliced into sections of about 20-25 nm in thickness with a diamond knife. The sectioned specimens were collected onto 400 mesh copper grids and observed at 100 kV of accelerating voltage using a transmission electron microscope (JEM 1210).

Results and Discussion

Capacitive parameter in equivalent circuit. The spectra of natural Al_2O_3 film produced in humid air were recorded at open-circuit potential (-1237 mV) in frequencies from $f_{\min} = 10$ mHz to $f_{\max} = 1$ MHz.

The measured impedance spectrum can be analyzed by using the simple equivalent circuit in Figure 1. In the circuit model, which consists of two impedance elements, Faradaic impedance and electrolyte resistance can be described in terms of resistance and layer impedance in terms of capacitance. But for fitting impedance spectra of passive metal electrode with variable stoichiometry¹⁶ a model with Young impedance (Figure 1 model B) instead of pure capacitance (Figure 1 model A) was used.

The physical meaning of Young impedance¹⁶⁻¹⁸ is based on a oxide layer with behavior of nonideal capacitor. The oxide layer is properly described by a dielectric layer of surface area A , thickness d and dielectric constant ε with a vertical decay of conductivity

$$\sigma_{Y(x)} = \sigma_{Y(x=0)} [1 - \exp(-x/d_0)] \quad (2)$$

in an outer zone of effective thickness d_0 . Figure 2 shows the impedance behavior results of Young impedance for the oxide layer, which is dependent on gradient profile of an exponentially decaying conductivity.

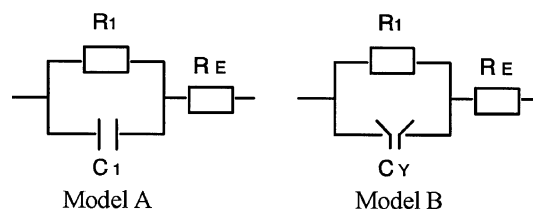


Figure 1. Electrical equivalent circuits with ideal capacitance (Model A) and with Young impedance (Model B) for fit of oxide layer.

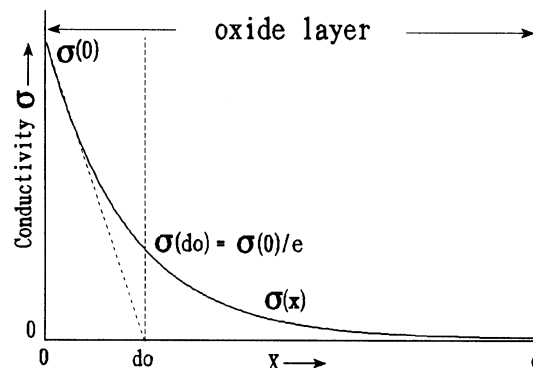


Figure 2. Schematic representation of surface layer with conductance gradients. An inhomogeneous dielectric of thickness d with exponential decay of the conductivity σ , penetration depth d_0 , relative penetration depth $p = d_0/d$.

Its impedance^{16,18} depends on three parameters: capacitance C_Y , relative penetration depth p and time constant τ , according to the following expression,

$$Z_Y = \frac{p}{i\omega C_Y} \ln\left(\frac{1 + i\omega \exp(p^{-1})}{1 + i\omega \tau}\right), \quad (3)$$

where $C_Y = \varepsilon_o \varepsilon A/d$, $p = d_0/d$, $\tau = \varepsilon_o \varepsilon(0)/\sigma(0)$ (4)

In these equations C_Y is the capacitance of the oxide layer, ε is the dielectric constant for aluminium oxide, ε_o is the permittivity of free space ($\varepsilon_o = 8.85 \times 10^{-12}$ F/m), A is the surface area, d is the thickness of the oxide, and $\sigma(0)$ is conductivity at the metal-oxide interface.

In the dielectric of the capacitor with a vertical gradient of the conduction in the direction x , the local time constant $\tau(x)$ at a distance x from the surface depends on only the local dielectric constant $\varepsilon(x)$ and the local conductivity $\sigma(x)$, according to

$$\tau(x) = \varepsilon_o \varepsilon(x) / \sigma(x), \quad (5)$$

which increases from outside to inside. At the border surface ($x=0$), according to Eq. (5), the time constant represent $\tau = \varepsilon_o \varepsilon(0) / \sigma(0)$ in Eq. (4). If $p (=d_0/d)$ is the relative penetration depth of the conduction in the layer of the total thickness d , then σ at $x = d_0$ is decayed to $\sigma(d_0) = \sigma(0)/e$. According to Eq. (3), Young impedance converges with decreasing frequency asymptotically to a resistance^{14,18}:

$$\lim_{\omega \rightarrow 0} Z_Y = R_Y = \frac{\tau p}{C_Y} (\exp(1/p) - 1) \quad (6)$$

with increasing frequency to a capacitance.

$$\lim_{\omega \rightarrow 0} Z_Y = \frac{1}{i\omega C} \quad (7)$$

The impedance characteristics of equivalent circuit model A, B in Figure 1 can be described and the circuit model A shows a frequency dependent impedance, Z_A , by Eq. (8).

$$Z_A = R_E + \left(\frac{R_1}{1 + (2\pi f \cdot R_1 \cdot C_1)^2} - \frac{1 + 2\pi f \cdot R_1^2 \cdot C_1}{1 + (2\pi f \cdot R_1 \cdot C_1)^2} \right) \quad (8)$$

However, the impedance of circuit model B can be determined by frequency range. At very low frequencies, the circuit impedance from Eq. (6) is given in Eq. (9).

$$Z_B = R_E + (R_Y^{-1} + R_1^{-1})^{-1} \quad (9)$$

But in higher frequency ranges, the circuit impedance from Eq. (7) can be described by the Eq. (10).

$$Z_B = R_E + \left(\frac{R_1}{1 + (2\pi f \cdot R_1 \cdot C_Y)^2} - \frac{i2\pi f \cdot R_1^2 \cdot C_Y}{1 + (2\pi f \cdot R_1 \cdot C_Y)^2} \right) \quad (10)$$

The natural Al_2O_3 film produced in humid air. The electrochemical behavior of this oxide layer can be described by simple equivalent circuit B with Young impedance.

Figure 3 shows fit results between the circuit model with Young impedance and normal capacitance for experimental

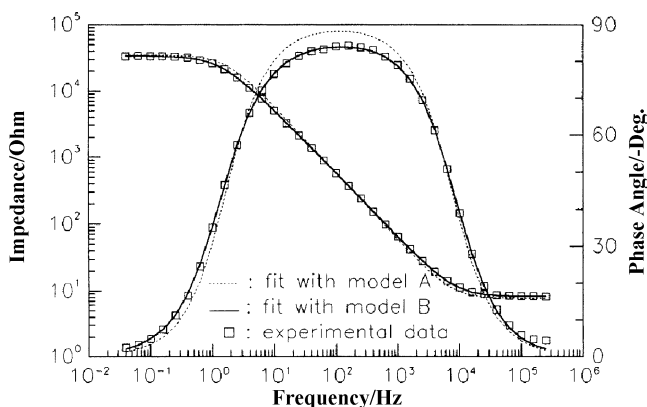


Figure 3. Fit results between circuit model with Young impedance and normal capacitance for experimental impedance spectrum of Al_2O_3 layer formed in humid air

Table 1. Evaluated impedance parameter according to equivalent circuit A, B and C for a spectrum of various oxide layer on Al at open-circuit potential in 0.5 M K_2SO_4 at 25 °C

Condition of layer	E_0 mV	C_b nF/cm ²	R_1 Ω	C_Y F/cm ²	p %	τ s	R_2 Ω	C_2 nF/cm ²	R_E Ω
1. natural passive layer in humid air	-1237	-	35k	2.2μ	3.7	4.5μ	-	-	8.2
2. anodized Al oxide layer (barrier type) formed in ammonium adipate solution	-39	-	1.3G	38.8n	1.6	1.3μ	-	-	6.9
3. anodized porous Al oxide layer formed	184	713	47M	527n	3.3	11n	30	108	8.9

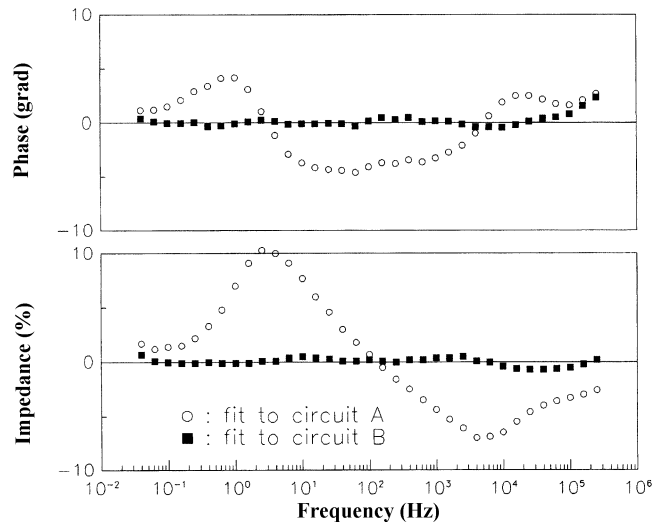


Figure 4. Comparison of fitting quality of the two equivalent circuit for a spectra of Al_2O_3 layer formed naturally in humid air on pure Al. Deviation plots for fitting of the spectrum with circuit A (○) and with circuit B (●).

impedance spectra of natural passive on aluminium. The deviations between the measured and fitted values of the impedance modulus (in dZ/Z , $(Z_{mea} - Z_{calc})/Z_{calc} \times 100\%$) and phase angle (in $dW(\text{grad})$, $W_{mea} - W_{calc}$) were plotted in Figure 4 for each of the experimental frequency values. The large deviations for the impedance and the phase angle in the fit results of circuit A, indicate that model A in Figure 1 does not match the experimental data. Much better agreement is observed when the same data are fitted to model B with Young impedance. These results show that for fitting impedance spectra of Al_2O_3 layer with the gradient profile of an exponentially decaying conductivity the equivalent circuit model with Young impedance (model B in Figure 1) instead of capacitance (model A in Figure 1) is suitable. Table 1 summarizes the evaluated impedance parameters for Al_2O_3 layers by circuit model.

The simulated data in Table 1 indicate that the resistance of the oxide layer is 35 kΩ and the capacitance of Al_2O_3 is 2.2 μF/cm². From capacitance of oxide layer on Al the thickness of the Al_2O_3 is calculated by using the conventional equation, as given in

$$d_{ox} = \epsilon \epsilon_0 A r / C_Y \quad (11)$$

where d_{ox} is the thickness of the barrier Al_2O_3 layer, C_Y is the capacitance of the oxide layer, A is the surface area, r is the

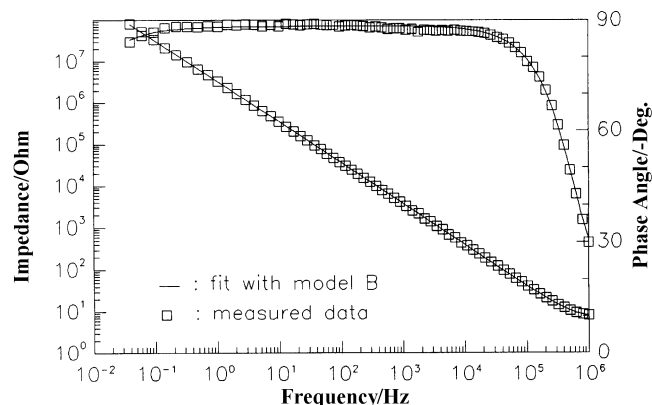


Figure 5. Impedance plot of fitted data point with model B on experimental impedance data for a spectra of barrier and compact oxide layer prepared in ammonium adipate ($\text{NH}_4\text{OCO}(\text{CH}_2)_4\text{COONH}_4$) solution.

geometrical surface area factor. Taking $\epsilon = 8.5$ for Al_2O_3 ,¹⁹ we estimated the thickness of oxide layer to be 3.42 nm (34.2 Å).

Barrier type oxide layer prepared in ammonium adipate. The impedance spectra were made at open-circuit potential (-39 mV) in 0.5 M K_2SO_4 solution and the frequency range from 10 mHz to 1 MHz. The impedance spectra and fitted result of barrier oxide layer produced artificially in ammonium adipate solution are shown in Figure 5.

The equivalent circuit used for the fit is given in model B in Figure 6. The electrochemical properties of the layer corresponds to that of an equivalent circuit containing two branches. One branch can be associated with the bulk resistance of the oxide layer and the other with the capacitive component of the passive layer, which behaves like an inhomogeneous dielectric as discussed above. By optimization of the parameters it is possible to estimate the thickness of the layer, the relative penetration depth and electric properties. From Young capacitance in Table 1, the thickness of the Al_2O_3 is calculated using equation (11). If the dielectric constant is assumed to be $\epsilon = 8.5$,¹⁹ the thickness of oxide can be determined to be 193 nm.

To obtain a reasonable interpretation of impedance spectra the barrier type oxide layer was examined by transmission electron microscopy (TEM). Figure 7 shows the TEM micrograph of a cross section of the oxide film formed on Al in 65 °C ammonium adipate solution (150 g/L) at 130V for 15 min. From the figure, the barrier type oxide film of dense and uniform thickness was estimated to be ca. 190 nm. This thickness is in agreement with the thickness (193 nm) of a barrier type oxide layer determined by interpretation of impedance spectroscopy.

According to Kuznetsova,¹⁹ the natural Al oxide growth in the humid air contrasts with the formation of oxide layer in ammonium adipate solution. In air the oxygen atoms chemisorbed on the aluminum surface form islands as a result of attractive force at island edges. With higher exposures the surface becomes covered completely and the oxidation mechanism, producing a thicker oxide film in a more com-

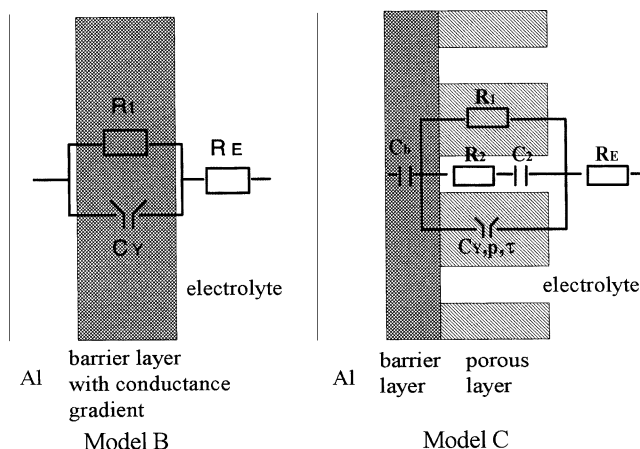


Figure 6. Equivalent circuit models for artificially formed Al_2O_3 layer. Circuit model B for barrier oxide layer formed in ammonium adipate and circuit model C for porous oxide layer formed in sulfuric acid.

plicated process, controlled by the gradients in chemical and electrical potentials. Furthermore, the growth of oxide layer on Al in air may lead to a relatively nondense film structure with defects and micropores.

The differences in the properties of oxide films account for the greater resistance of the barrier type film formed in ammonium adipate solution; 1.3 GΩ compared with the resistance of oxide layer grown in air, 35 kΩ (Table 1).

Porous oxide layer formed in sulfuric acid. The aluminium oxide formed from anodizing in sulfuric acid has a complex form.²⁰⁻²³ It is partially hydrated and has a two layer structure. At the surface of the metal there is a thin, compact boundary layer (barrier type layer) and then there is a porous overlayer. The latter has a very open structure. For complex oxide layer, a modified circuit (Figure 6-b) was used for the fit. The fitted results with equivalent circuit C in Figure 8 show the good agreement with the experimental impedance spectrum for porous oxide layers of Al.

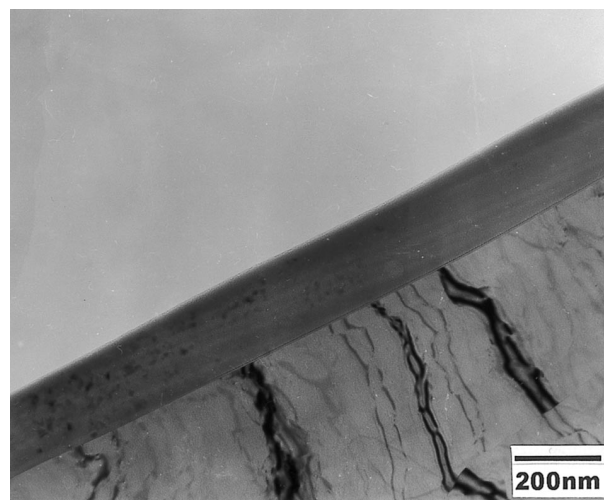


Figure 7. Transmission electron micrograph of the cross section of the barrier type oxide film formed in ammonium adipate electrolyte.

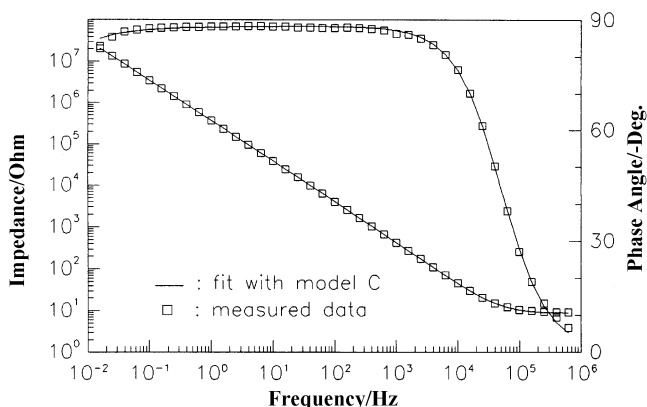


Figure 8. Impedance plot of fitted data point with model C on experimental impedance data for a spectra of porous oxide layer anodized in 1M sulfuric acid.

The circuit for fit in Figure 6 (model C) consists of six impedance elements with a total of eight parameters. The three parallel branches for a porous layer in series to a capacity C_b , which represents the capacitance of the inner barrier layer, are connected in series to a resistor R_E that is correlated with the resistance of the electrolyte. The parameters R_1 and C_Y can be associated with the resistance for porous structure layer. The parameters of R_2 and C_2 can be correlated with the resistance of electrolyte inside the pores and the double layer of the inner pore surfaces, respectively.

The evaluated impedance parameters for Al_2O_3 layers by circuit model are summarized in Table 1. The capacitance C_b of the inner barrier oxide layer is 713 nF/cm^2 , which suggests a barrier layer thickness of $0.01 \mu\text{m}$ by Eq. (11). The resistance R_1 of outer oxide layer, $47 \text{ M}\Omega$, represents low conductivity property; the capacitance C_Y is represented by 527 nF/cm^2 . In this outer oxide layer, the pores are probably filled only with the solution. Because of this open porous outer structure, it is difficult to calculate the thickness of the outer layer from the C_Y values.²³ Since the outer Al_2O_3 layer seems to be thick and the pores are filled with solution, the contribution to electrochemical properties and the impedance response are largely from this porous layer.

Conclusion

The impedance characteristics for both artificially produced Al_2O_3 and naturally formed passive layer on pure Al substrate have been studied by using electrochemical impedance spectroscopy.

To represent the impedance characteristics of the barrier type Al oxide, a quite simple equivalent circuit was sufficient. It consisted of a parallel circuit with Young impedance C_Y and the bulk resistance of the oxide layer R_1 in series to a resistance R_E , representing the electrolyte. But for oxide layer formed in sulfuric acid, a modified circuit based on a complex twolayer oxide consisting of inner barrier layer and outer porous layer was used for the fit.

The electrochemical parameters of Al_2O_3 layers are correlated with the properties and morphologies of the oxide layer. The oxide layer formed in ammonium adipate solution exhibits a relatively uniform and dense film structure, leading to the greater oxide layer resistance, compared with naturally formed passive layer in air.

The electrochemical behavior of Al_2O_3 layers with variable stoichiometry can be monitored by evaluating an equivalent circuit with Young impedance, which converges with increasing frequency asymptotically to an ideal capacitance and can be described as an imperfect capacitance with the gradient profile of an exponentially decaying conductivity instead of ideal capacitance.

References

1. Wernick, S.; Pinner, R.; Sheasby, P. G. *The Surface Treatment and Finishing of Aluminum and Its Alloy*, ASM and Finishing Publication Ltd.: 1987; Vol.1, p 303.
2. Ginsberg, H.; Caden, W. *Aluminum development Assoc. Conference on Anodizing*; Nottingham, 1961; No.8, p 101.
3. Hunter, M. S.; Towner, P. F. *J. Electrochem. Soc.* **1961**, *108*, 139.
4. Hufnagel, W. In *Aluminium-Taschenbuch*; Aluminium-Verlag: Duesseldorf, 1988; p 170.
5. Uhlig, H. H.; Revie, R. W. *Corrosion and Corrosion Control*; John Wiley & Sons: 1985; p 341.
6. Hoar, J. P.; Wood, G. C. *Electrochim. Acta* **1962**, *7*, 333.
7. Koda, M.; Takahashi, H.; Nagayama, M. *Kinzoku Hyomen Gijutsu* **1982**, *33*, 1.
8. Koda, M.; Takahashi, H.; Nagayama, M. *34th Meeting of Int. Soc. Electrochem., Ext. Abstracts*; Erlangen, Germany, 1983; p 803.
9. Jason, A. C.; Wood, G. C. *Proceedings of the Physics Society, London* **1955**, *B(68)*, 1105.
10. Grundner, M.; Halbritter, J. *J. Appl. Phys.* **1980**, *51*, 397.
11. Gray, K. E. *Appl. Phys. Lett.* **1975**, *27*, 462.
12. Goehr, H.; Schaller, J.; Schiller, C.-A. *Electrochim. Acta* **1993**, *38*, 1961.
13. Mansfeld, F. *Corrosion Science* **1988**, *44(8)*, 558.
14. Göhr, H. *Ber. Bunsenges. Phys. Chem.* **1981**, *85*, 274.
15. Göhr, H. *Z. Physik. Chem. N. F.* **1986**, *148*, 105.
16. Young, L. *Anodic Oxide Films*; Academic Press: New York, 1961; p 253-267.
17. Young, L. *Faraday Soc.* **1955**, *51*, 1250.
18. Göhr, H.; Oh, H.-J.; Schiller, C.-A. *GDCh-Monographie Band2* **1995**, 341.
19. Kuznetsova, A.; Burleigh, T. D.; Zhukov, V.; Blachere, J.; Yates, Jr. J. T. *Langmuir* **1998**, *14(9)*, 2502.
20. Keller, F.; Hunter, M. S.; Robinson, D. L. *J. Electrochem. Soc.* **1953**, *100*, 411.
21. Patermarakis, G. *J. Electroanal. Chem.* **1998**, *447*, 25.
22. Hitzig, J.; Juettner, K.; Lorenz, W. J.; Paatsch, W. *Corrosion Science* **1984**, *24*, 945.
23. Mansfeld, F.; Zhang, G.; Chen, C. *Plating & Surface Finishing* **1997**, *Dec*, 72.
24. Pan, H.; Thierry, D.; Leygraf, C. *Electrochim. Acta* **1996**, *41*, 1143.